STEADY-STATE AND DYNAMIC MASS TRANSFER OF GASES IN POROUS MATERIALS*

Axel TUCHLENSKI[1], Oliver SCHRAMM[2] and Andreas SEIDEL-MORGENSTERN[3,**]

Institut für Verfahrenstechnik, Otto-von-Guericke Universität Magdeburg, 39106 Magdeburg, Germany; e-mail: [1]axel.tuchlenski@masch-bau.uni-magdeburg.de, [2]oliver.schramm@masch-bau.uni-magdeburg.de, [3]andreas.seidel-morgenstern@masch-bau.uni-magdeburg.de

Received October 15, 1996
Accepted January 27, 1997

The diffusion of binary gas mixtures through a porous asymmetric tubular membrane has been studied experimentally. A modified Wicke–Kallenbach diffusion cell consisting of two gas compartments separated by the membrane was used. Steady-state experiments with pure gases and binary mixtures were carried out in order to determine the transport parameters of the membrane with respect to the dusty gas model. To verify these parameters, the dynamic transport of binary mixtures was examined applying the dynamic diffusion cell technique proposed by Novák *et al.* The measured transients were in relative good agreement with the model predictions.

Key words: Porous membrane; Dusty gas model; Diffusion experiments; Dynamic diffusion cell technique.

To design and optimize catalytic reactors, fixed-bed adsorbers and membrane separation processes, a proper description of the multicomponent mass transfer in porous materials is essential. Several concepts and correlations for predicting this transfer have been developed. However, the deviations between the predicted fluxes and the experimentally observed data occasionally reach orders of magnitude[1]. At present, experiments are considered to be the only alternative to determine the reliable multicomponent diffusivities describing the mass transfer in porous media.

On studying the multicomponent diffusion and chemical reaction within catalyst pellets, Krishna[2] pointed out that the standard formulation of diffusion processes based on Fick's law frequently fails even on a qualitative level and that the more general Stefan–Maxwell formulation provides a better tool to describe intraparticle diffusion. Based on the latter approach, the dusty gas model was proposed by Mason and Malinauskas[3].

* Presented at the *Symposium on Diffusion in Zeolites and Other Microporous Materials at the twelves CHISA'96 Congress, Prague, August 25–30, 1996.*

**The author to whom correspondence should be addressed.

The objective of this paper is to test the capability of the dusty gas model for the prediction of multicomponent diffusion effects in a porous asymmetric tubular membrane. Therefore, the combination of steady-state and transient diffusion experiments was applied. The performed steady-state measurements are based on the well-known Wicke–Kallenbach method. For the transient experiments, the dynamic diffusion cell technique proposed by Novák *et al.*[4] was adapted.

THEORETICAL

Mass transfer in porous systems is considered to be based mainly on four different mechanisms. According to Mason and Malinauskas[3], these most important transport resistances in porous systems can be illustrated in analogy to an electric circuit as shown in Fig. 1. The following contributions can be distinguished:

– Diffusive mass transfer (J_i^D)

The diffusive mass transfer is considered to occur by the molecular diffusion in large pores and by the Knudsen diffusion in smaller pores. In the theory of Bosanquet[5] it is assumed that the combination of these processes can be described by one averaged effective diffusivity.

– Viscous flux (J_i^V)

An overall pressure gradient causes a convective mass transfer through the porous matrix.

– Surface diffusion (J_i^S)

Adsorbed molecules might possess a certain mobility which leads to a flux along the surface in the direction of the adsorbed phase concentration gradient.

For the total molar flux,

$$J_i = J_i^D + J_i^V + J_i^S \qquad (1)$$

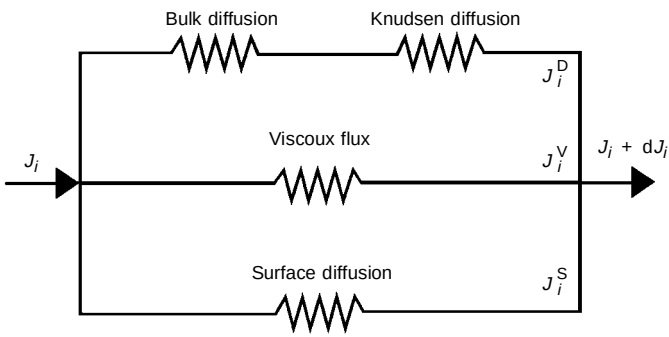

FIG. 1
Electric analogue circuit monitoring the transport resistances in porous solids

holds. In the following, the effect of surface diffusion will be neglected ($J_i^S \approx 0$) because only weakly adsorbable inert gases have been used in the experiments described below.

The simplest attempt to describe the diffusive fluxes J_i^D in a multicomponent mixture is given by Fick's law. When an overall pressure gradient over the porous solid occurs, the contribution of the viscous flux can be taken additively into account using d'Arcy's law. Then, one obtains for the total molar flux of species *i*:

$$J_i = J_i^D + J_i^V = -\frac{1}{\boldsymbol{R}T}\left(D_i^e \nabla p_i + \frac{B_0}{\eta} x_i\, p \nabla p\right), \quad i = 1, N \ . \tag{2}$$

According to the law of Bosanquet[5], the calculation of the effective diffusivity D_i^e for a species *i* in the transition region is based on the effective mixture bulk diffusivity $D_{i,m}^e$ and the effective Knudsen diffusivity $D_{K,i}^e$.

$$\frac{1}{D_i^e} = \frac{1}{D_{i,m}^e} + \frac{1}{D_{K,i}^e} \tag{3}$$

An estimate of the effective mixture bulk diffusivity can be calculated from Blanc's law (see Reid *et al.*[6]) based on the binary molecular diffusivities D_{ij}^0 and composition:

$$D_{i,m}^e = \frac{\varepsilon}{\tau}\left(\sum_{j=1, j\neq i}^{N} \frac{x_j}{D_{ij}^0}\right)^{-1} \ . \tag{4}$$

For the Knudsen diffusivity,

$$D_{K,i}^e = \frac{4}{3} K_0 \left(\frac{8\boldsymbol{R}T}{\pi M_i}\right)^{1/2}, \quad \text{with } K_0 = \frac{\varepsilon}{\tau}\frac{d_p}{4} \tag{5}$$

holds. In the equations above, ε/τ is the ratio of porosity to tortuosity, K_0 is the Knudsen coefficient which is related to the mean pore diameter d_p of the porous solid and B_0 is the permeability constant of the porous medium.

Mutual kinetic interactions in multicomponent systems usually influence the mass transfer more significantly than predicted by Fick's law, Eqs (*2*)–(*5*). An alternative possibility of taking the interactions into account is to relate the diffusive mass transfer of a component to the partial pressure gradients of all other components present in the mixture by introducing cross diffusivities D_{ij}^e. However, attempts to apply this extended version of Fick's law have shown that such additional coefficients might be strongly concentration dependent and take even negative signs[2].

In order to describe multicomponent diffusion processes in a bulk phase, the application of the Stefan–Maxwell theory instead of Fick's law is straightforward[2]. The dusty gas model (DGM) is one suitable approach to combine the Stefan–Maxwell diffusion equations with the characteristics of mass transfer in a porous solid[3,7]. Its basic idea is

to consider the solid as a matrix of single fixed dust molecules. These dust molecules form an additional pseudospecies with an infinite molecular weight. With respect to the kinetic gas theory, momentum is assumed to be transferred by elastic binary collisions among all different pairs of molecules. The advantage of this approach is that frictional drag effects caused by motion of other components can be taken directly into account. The viscous contribution J_i^V can also be incorporated. The flux for a single species *i* in a multicomponent mixture is expressed by the DGM according to the following equation[3]:

$$\sum_{j=1,j\neq i}^{N} \frac{x_j J_i - x_i J_j}{\frac{\varepsilon}{\tau} D_{ij}^0} + \frac{J_i}{D_{K,i}^e} = -\frac{p}{RT}\nabla x_i - \frac{x_i}{RT}\left(1 + \frac{B_0}{\eta D_{K,i}^e} p\right)\nabla p , \quad i = 1, N \ . \tag{6}$$

Assuming the porous solid to be homogeneous, the DGM contains, in combination with Eq. (5), three structural parameters K_0, B_0, and ε/τ which have to be determined experimentally. These structural parameters are solely related to the porous solid characteristics and do not depend either on the gas type or the process conditions. A more detailed mathematical model for the gas permeation in asymmetric membranes taking heterogeneous porous structures into account was developed by Uchytil[8]. This model is based on the separate determination of structural parameters of the membrane support and the top layer, respectively. Nevertheless, the simplifying assumption of homogeneity is often deemed to be fulfilled in order to determine integral parameters[4] and was applied below.

In the following an experimental method for the determination and verification of the three mentioned structural parameters will be presented.

EXPERIMENTAL

A tubular asymmetric Al_2O_3 membrane was used in the experiments. The top layer consists of TiO_2. The membrane was supplied by Cerasiv GmbH (Plochingen, Germany). Figure 2 is a SEM photograph of

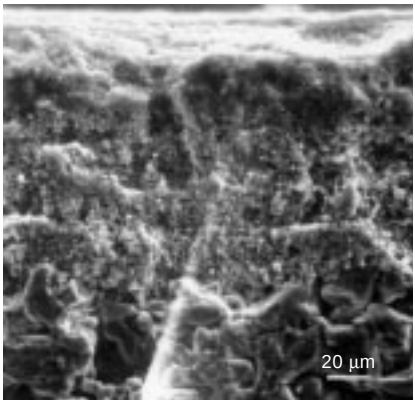

FIG. 2
SEM photograph of the membrane (zoom factor 500), upper part: top layer (≈ 20 μm)

the membrane in which three successive layers can be recognized. The thickness of the top layer can be estimated to be approximately 20 μm. The corresponding mercury porosigram of the membrane is given in Fig. 3. It can be seen that a multimodal pore size distribution is present. According to this distribution curve, the top layer of the membrane consists of macropores with a mean pore diameter of 130 nm. Due to relatively large pore diameters within the support (≈ 5 000 nm) and the intermediate layer (≈ 500 nm), the entire transport resistance of the membrane was related in the following to the top layer. The textural properties of the membrane are summarized in Table I.

For the determination of the three structural parameters, a diffusion cell of the Wicke–Kallenbach type was applied. The experimental set-up is shown in Fig. 4. Compared to the conventional Wicke–Kallenbach method, the set-up was arranged in such a way that the outer volume of the diffusion cell

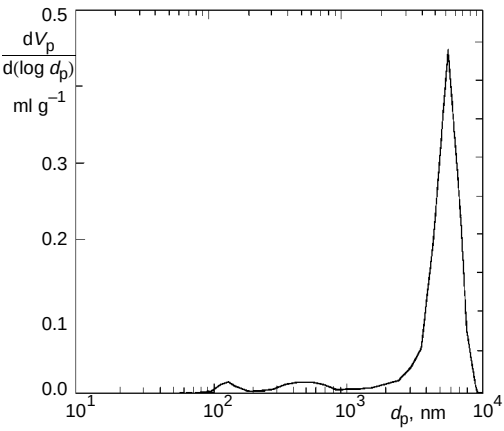

FIG. 3
Pore size distribution of the membrane obtained from mercury porosimetry

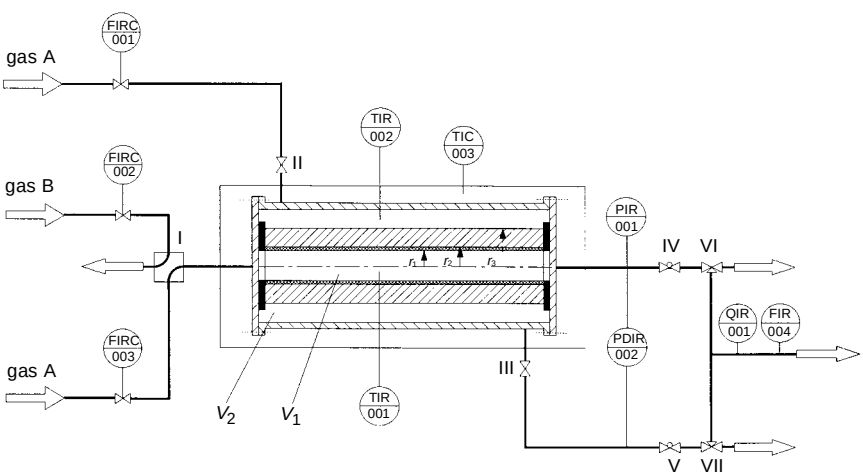

FIG. 4
Experimental set-up for the steady-state and transient diffusion experiments: FIRC 001–003 mass flow controller, FIR 004 soap-film flow-meter, TIR 001–002 thermocouple, TIC 003 temperature control, PIR 001 pressure gauge, PDIR 002 difference pressure gauge, QIR 001 thermal conductivity detector, I four-way valve, II–III shutt-off valve, IV–V needle valve, VI–VII three-way valve

could be closed by two valves. The cell was made of stainless steel. Two gas volumes are separated by the tubular porous membrane. The inner volume is given by the membrane geometry (i.d. 7 mm, o.d. 10 mm, length 100 mm). The outer annular volume of the cell V_2 is approximately 65 ml. The sealings between the two compartments consist of graphite rings. Thermocouples were used to determine the temperatures in both the volumes. A furnace was provided for temperature control up to 500 K. The flow rates at the inlet were measured and controlled by mass flow controllers. The outlet flow rates were measured with soap-film flow-meters. To read the absolute pressure in the inner volume, a pressure gauge was installed at the outlet. Further, the pressure difference over the membrane was measured. Gas compositions were determined by applying a thermal conductivity detector. Due to the flexibility of the experimental set-up, three different types of experiments could be carried out:

1. In a steady-state permeation experiment, both the volumes were fed with the same gas. Adjusting a pressure difference over the membrane with the two needle valves, a transmembrane flux was induced. By measuring the pressure in the inner volume as well as the pressure difference and the volumetric flow rates at the outlets, the transmembrane molar flow rate can be calculated from a mass balance.

2. A binary diffusion experiment was carried out under steady-state and isobaric conditions. Therefore, the outer volume was supplied with gas A and the inner volume with gas B. Due to the isobaric conditions, the mass transfer is purely diffusive. To calculate the transmembrane molar flow rates of gas A and B, the volumetric flow rates and gas compositions at both outlets were measured.

3. To characterize the transient diffusion behavior of a binary gas mixture, the outer gas volume of the diffusion cell was closed. Before starting the experiments, the inner volume of the diffusion cell was rinsed with gas A until the whole system reached steady state. Then, the four-way valve was switched to supply gas B to the inner volume, and the response of the pressure in the outer volume was detected recording the pressure difference between inner and outer volume.

RESULTS AND DISCUSSION

For the analysis of the diffusion experiments described below, the relation between the diffusive fluxes, J_i, and the experimentally accessible transmembrane molar flow rates, $\dot{n}_i^{12}$, is required. For a differential slice of a tubular membrane the relation

$$\mathrm{d}\dot{n}_i^{12} = J_i(r)\, 2\pi r\, \mathrm{d}z = \bar{J}_i(r_\mathrm{M})\, 2\pi r_\mathrm{M}\, \mathrm{d}z\,, \qquad i = 1, N \tag{7}$$

TABLE I
Textural properties of the membrane

Parameter	Value
BET specific surface, $m^2\ g^{-1}$	0.151
Apparent density[a], $g\ cm^{-3}$	3.85
Specific pore volume[a], $cm^3\ g^{-1}$	0.108
Porosity[a]	0.293

[a] From mercury porosimetry.

holds. Under steady-state conditions, the flow rates $\dot{n}_i^{12}$ are constant, and it is expedient to define an averaged transmembrane flux, $\bar{J}_i$, related to the mean radius, $r_M = (r_1 + r_2)/2$. Using this averaged transmembrane flux and linearized forms of the radial derivatives the DGM, Eq. (*6*), becomes:

$$\sum_{j=1,j\neq i}^{N} \frac{x_j\bar{J}_i - x_i\bar{J}_j}{\frac{\varepsilon}{\tau}D_{ij}^0} + \frac{\bar{J}_i}{D_{K,i}^e} = -\frac{p}{\boldsymbol{R}T}\frac{\Delta x_i}{r_M \ln(r_2/r_1)} - \frac{x_i}{\boldsymbol{R}T}\left(1 + \frac{B_0}{\eta D_{K,i}^e}p\right)\frac{\Delta p}{r_M \ln(r_2/r_1)}, \quad i = 1, N . \quad (8)$$

This equation will be used in subsequent evaluation of the experimental data.

Results of the Permeation Experiment 1

On applying the following mass balances, the transmembrane molar flow rate $\dot{n}_i^{12}$ of a single gas *i* can be calculated from the experimentally determined p_1, p_2, $\dot{V}_1$, $\dot{V}_2$:

$$-\frac{p_1}{\boldsymbol{R}T}(\dot{V}_1 - \dot{V}_1^0) = \frac{p_2}{\boldsymbol{R}T}(\dot{V}_2 - \dot{V}_2^0) = \dot{n}_i^{12} . \quad (9)$$

The integrated form of Eq. (*7*) delivers $\bar{J}_i = \dot{n}_i^{12}/2\pi r_M L$. According to Eq. (*8*), the linearized DGM for a single gas leads to:

$$\bar{J}_i = -\frac{1}{\boldsymbol{R}T}\left(D_{K,i}^e + \frac{B_0(p_1 + p_2)}{2\eta}\right)\frac{\Delta p}{r_M \ln(r_2/r_1)} . \quad (10)$$

Consequently, the ratio $\bar{J}_i/\Delta p$ should be proportional to the average pressure $(p_1 + p_2)/2$ in the membrane according to:

$$\frac{\bar{J}_i}{\Delta p} = -\frac{1}{\boldsymbol{R}T}\left(D_{K,i}^e + \frac{B_0(p_1 + p_2)}{2\eta}\right)\frac{1}{r_M \ln(r_2/r_1)} . \quad (11)$$

From a corresponding plot, $D_{K,i}^e/r_M \ln(r_2/r_1)$ and $B_0/r_M \ln(r_2/r_1)$ can be determined. To estimate explicit values for the Knudsen diffusivity and the permeability constant, it is required to specify a diffusion path length. This estimation was performed relating the entire transport resistance of the membrane arbitrarily to the top layer (thickness approximately 20 μm, r_1 = 3.5 mm, r_2 = 3.52 mm). Using the calculated Knudsen diffusivities $D_{K,i}^e$, the values for K_0 can be obtained from Eq. (*5*). Figure 5 shows the permeation characteristics of the membrane observed for four different gases. All values for K_0 and B_0 obtained from the permeation data for different gases should be identical. Assuming ideal cylindrical pores, the mean pore diameter of the membrane can be estimated[3] as

$$d_p = \frac{8B_0}{K_0} \quad . \tag{12}$$

Table II summarizes the results of experiment *1* for four different gases. Within the frame of experimental accuracy, the derived values for K_0 show a relative good agreement. The deviations for B_0 are higher than for K_0. This can be attributed to the fact that B_0 is related to the variance of the pore size distribution whereas K_0 is proportional to the average of the pore diameter[3].

Results of the Steady-State Diffusion Experiment 2

To quantify the third structural parameter ε/τ, the isobaric binary diffusion experiment *2* was carried out. To analyze the results, the following mass balance equations of species *i* in the two gas compartments 1 and 2 have been solved:

$$\frac{p}{\boldsymbol{R}T}\frac{\mathrm{d}(\dot{V}_1 x_{1,i})}{\mathrm{d}z} = -2\pi r_M \bar{J}_i \quad , \quad i = 1, 2 \quad , \tag{13}$$

$$\frac{p}{\boldsymbol{R}T}\frac{\mathrm{d}(\dot{V}_2 x_{2,i})}{\mathrm{d}z} = 2\pi r_M \bar{J}_i \quad , \quad i = 1, 2 \quad . \tag{14}$$

The boundary conditions for Eqs (*13*) and (*14*) are:

$$z = 0: \quad \dot{V}_1(0) = \dot{V}_1^0; \quad x_{1,i}(0) = 1; \quad \dot{V}_2(0) = \dot{V}_2^0; \quad x_{2,i}(0) = 0 \quad . \tag{15}$$

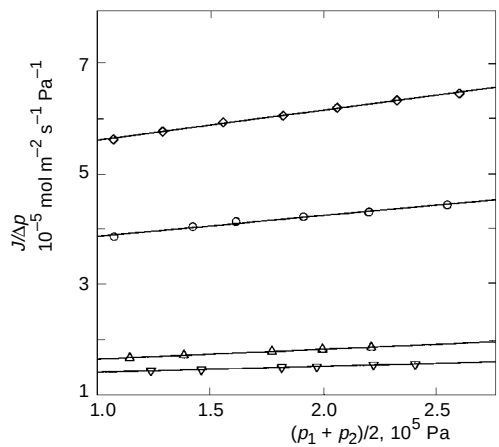

FIG. 5
Permeation of single gases through the membrane at 293 K: ✧ H_2, ❍ He, Δ N_2, ∇ Ar

In order to achieve the averaged transmembrane flux $\bar{J}_i$, the linearized DGM, Eq. (*8*), was reduced to the isobaric case:

$$\sum_{j=1,j\neq i}^{N=2} \frac{x_j\bar{J}_i - x_i\bar{J}_j}{\varepsilon/\tau} \frac{D^{e}_{K,i}}{D^{0}_{ij}} + \bar{J}_i = -\frac{p}{\boldsymbol{R}T} \frac{D^{e}_{K,i}\Delta x_i}{r_M \ln (r_2/r_1)} \quad , \qquad i = 1, 2 \ . \tag{16}$$

Applying an ODE solver of the Runge–Kutta type, the numerical integration of Eqs (*13*)–(*16*) allows the determination of the mole fractions and the volumetric flow rates at the diffusion cell outlets, respectively. For the numerical integration, the effective Knudsen diffusivities were calculated according to Eq. (*5*) with an averaged value of K_0 obtained in the experiments *1* and depicted in Table II. The D^0_{ij} values were taken from the literature[9] and can be found in Table III. The value for the ratio ε/τ was varied in subsequent numerical integrations of Eqs (*13*)–(*16*). On the basis of a least square fit, the theoretical results were matched to the experimental data by adjusting the ratio ε/τ. Table III gives the best values of the ratio ε/τ for different binary gas mixtures. The obtained values are similar for all experiments as required by theory.

TABLE II
Structural parameters resulting from the permeation experiments *1* at 293 K and pore diameter calculated from Eqs (*5*), (*11*) and (*12*): related to the top layer thickness

Gas	$K_0 \cdot 10^9$, m	$B_0 \cdot 10^{17}$, m^2	$d_p \cdot 10^9$, m
Ar	1.21	1.22	80.1
N_2	1.15	1.57	108.0
He	1.02	3.78	294.8
H_2	1.06	2.39	180.0
Average, %	1.11 ± 8	2.24 ± 51	166.4 ± 58

TABLE III
Molecular binary diffusivities[9] and the determined ratio of ε/τ resulting from the isobaric binary diffusion experiments *2* at 293 K

Gas pair	$D^0_{ij} \cdot 10^5$, m^2 s^{-1}	$\varepsilon/\tau \cdot 10^3$
H_2–N_2	7.72	1.64
He–N_2	6.98	1.59
Average, %		1.62 ± 2

It should be noted here that the ratios $D^{e}_{K,i}/r_M \ln(r_2/r_1)$ and $B_0/r_M \ln(r_2/r_1)$, available from experiment *1* determine entirely the contribution of the Knudsen diffusion and viscous flux to the transport resistance of the membrane. Only the specification of a diffusion path length delivers explicit values for $D^{e}_{K,i}$ and B_0 and subsequently for the ratio ε/τ.

Results of the Transient Diffusion Experiment 3

Considering the transient binary diffusion experiment *3*, a nonequimolar mass transfer through the membrane occurs if the exchanged gases A and B have different molecular weights. This effect is due to Graham's law:

$$\sum_{i=1}^{N=2} J_i \sqrt{M_i} = 0 \ . \qquad (17)$$

The nonequimolar diffusion fluxes through the membrane induce a pressure change in the closed outer volume V_2. This pressure change is caused by the difference between the ingoing and outgoing overall fluxes. The magnitude and direction of the pressure change depend on the ratio of the molecular weights of the two species, the membrane structure parameters, and the volumetric flow rate in the inner volume. In the course of time the pressure difference over the membrane is gradually compensated by a viscous flux. Assuming, for the sake of simplicity, ideally mixed conditions in the outer volume V_2, the corresponding total mass balance becomes:

$$\frac{1}{\boldsymbol{R}T}\frac{\partial p_2}{\partial t} = \frac{2\pi r_M}{V_2}\sum_{i=1}^{N=2}\int_0^L \bar{J}_i \, \mathrm{d}z \ . \qquad (18)$$

For the component mass balances in the outer volume further holds:

$$\frac{1}{\boldsymbol{R}T}\frac{\partial p_{2,i}}{\partial t} = \frac{2\pi r_M}{V_2}\int_0^L \bar{J}_i \, \mathrm{d}z \ , \quad i = 1, 2 \ . \qquad (19)$$

To achieve a more realistic description of the transient diffusion behavior, the axial gradients concerning the volumetric flow rate and the partial pressures in the inner volume were taken into account. Consequently, the overall mass balance and the component mass balances in the inner volume V_1 are:

$$\frac{1}{\boldsymbol{R}T}\frac{\partial p_1}{\partial t} = -\frac{1}{\boldsymbol{R}T}\frac{1}{q_1}p_1\frac{\partial \dot{V}_1}{\partial z} - \frac{2\pi r_M}{q_1}\sum_{i=1}^{N=2}\bar{J}_i = 0 \ , \qquad (20)$$

$$\frac{1}{\boldsymbol{R}T}\frac{\partial p_{1,i}}{\partial t} = -\frac{1}{\boldsymbol{R}T}\frac{1}{q_1}\frac{\partial(\dot{V}_1 p_{1,i})}{\partial z} - \frac{2\pi r_M}{q_1}\bar{J}_i \ , \quad i = 1, 2 \ . \tag{21}$$

As reflected in Eq. (*20*), it was assumed that the pressure p_1 in the inner volume remains constant. The averaged transmembrane flux $\bar{J}_i$ was derived using Eq. (*8*). It was assumed that the accumulation of species *i* within the gas phase of the membrane is negligible. This assumption is valid as long as the closed outer volume is large compared to the gas phase volume in the pores of the membrane.

To solve the system of differential equations, the method of lines was applied[10]. Therefore, at first a space discretization of Eqs (*20*) and (*21*) was carried out to obtain ordinary differential equations. Then, the semi-implicit Runge–Kutta ODE solver with adaptive step size[11] was used for the numerical integration over time. The initial and boundary conditions are:

$$t = 0: \ \ p_{1,i}(0, z > 0) = p_1 \ ; \ \ \dot{V}_1(0,z) = \dot{V}_1^0 \ ; \ \ p_{2,i}(0) = p_1 \ ; \ \ p_2(0) = p_2^0 = p_1 \ . \tag{22}$$

$$z = 0: \ \ p_{1,i}(t,0) = 0 \ ; \ \ p_1(t,0) = p_1 \ ; \ \ \dot{V}_1(t,0) = \dot{V}_1^0 \ . \tag{23}$$

The spatial mesh size was kept constant during the integration. To eliminate numerical dispersion effects, the mesh size was reduced in preliminary calculations successively until no further change in the results was observed. For the axial discretization, 120 grid points were found to be sufficient to obtain accurate results.

The dynamic diffusion behavior was studied for the binary system of argon and hydrogen. Initially, the cell was completely filled with Ar and at $t = t_0$ the feed flow to the

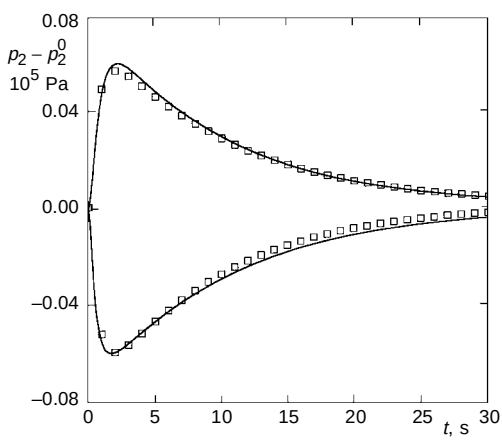

FIG. 6
Pressure response curves for the transient diffusion experiment with Ar and H_2 at 293 K. Upper curve: H_2 substitutes Ar. Lower curve: Ar substitutes H_2. Lines represent the model predictions from Eqs (*18*)–(*21*): $p_1 = p_2^0 = 10^5$ Pa, $\dot{V}_1^0 = 500$ cm^3 min^{-1}

inner volume was replaced by a H_2 stream. Hydrogen diffuses faster through the membrane and consequently a pressure increase in the outer volume can be detected. Figure 6 shows the pressure reponse as a function of time together with the model predictions. The reversed experiment, replacing H_2 by Ar, is also depicted in this figure. The transients were calculated using the three structural parameters obtained from the steady-state experiments. For the calculation of the mean mixture viscosity, Wilke's mixture rule[6] was applied. Mole fraction of 0.5 was assumed for each species.

In Fig. 6 a good agreement between the theory and experiment can be noticed. This is considered to be an independent prove for the validity of the obtained structural parameters. To study the diffusion dynamics at elevated temperatures, the same experiment was carried out at 423 K. The results are shown in Fig. 7. To simulate this experiment, only the binary diffusion coefficients and the viscosities were adapted[9]. The agreement between the model predictions and experimental data is also good. From all transients it can be concluded that the DGM is able to describe the dynamic mass transfer of binary gas mixtures through asymmetric porous membranes satisfactorily using the structural parameters determined from steady-state data.

Analyzing the results more critically, deviations for the reversed experiment (replacing H_2 by Ar) can be observed. One reason might be that the relative small transport resistance of the applied membrane leads to high transmembrane fluxes. As a consequence, a remarkable increase in the volumetric flow rate is caused at the beginning of the reversed experiment. Due to the increased volumetric flow rate, the time to exchange both gases decreases. This effect causes an asymmetry of the transients. In the experiment it was observed that due to the higher flow rates initially a slight pressure increase in the inner volume occurred. Therefore, the simplifying assumption of a constant total pressure p_1 in the inner volume, Eq. (*20*), was not perfectly fulfilled.

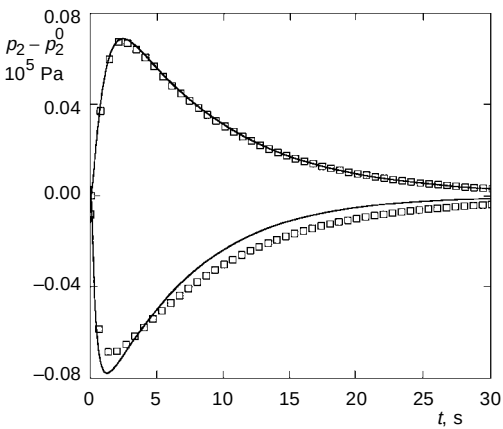

FIG. 7
Pressure response curves for the transient diffusion experiment with Ar and H_2 at 423 K. Upper curve: H_2 substitutes Ar. Lower curve: Ar substitutes H_2. Lines represent the model predictions from Eqs (*18*)–(*21*): $p_1 = p_2^0 = 10^5$ Pa, $\dot{V}_1^0 = 722$ cm^3 min^{-1}

CONCLUSIONS

To describe the transport of multicomponent mixtures through a porous asymmetric membrane, an experimental set-up was proposed allowing the combination of steady-state and dynamic measurements. Based on the dusty gas model, the three structural parameters of the membrane were obtained from permeation experiments with several nonadsorbable pure gases and from binary isobaric diffusion experiments. The determined parameters were in good agreement with the model assumptions.

For the verification of the experimentally derived parameters, a dynamic diffusion cell technique was applied similar to the set-up proposed by Novak *et al.*[4]. In the absence of surface effects, the dynamic nonisobaric transport of a binary mixture through the membrane was described satisfactorily by the dusty gas model using the parameters obtained from steady-state data.

For the quantification of mass transfer in porous media, the dynamic diffusion cell technique offers a promising experimental tool. The agreement or disagreement between the experimental and theoretical pressure response curves might give further information on the occurrence of other effects not considered by the DGM, as, *e.g.* surface diffusion or adsorption processes[12].

SYMBOLS

B_0	permeability constant, m^2
D_i	Fickian diffusivity, $m^2\ s^{-1}$
$D^0_{i,j}$	binary diffusivity in bulk fluid phase, $m^2\ s^{-1}$
$D_{K,i}$	Knudsen diffusivity of species i, $m^2\ s^{-1}$
d_p	pore diameter, m
J_i	diffusion flux of species i, mol $m^{-2}\ s^{-1}$
K_0	Knudsen coefficient, m
L	membrane length, m
M_i	molar weight of species i, g mol^{-1}
N	number of diffusing species
$\dot{n}_i$	molar flow rate of species i, mol s^{-1}
p	absolute pressure, Pa
Δp	pressure difference ($p_2 - p_1$), Pa
p_i	partial pressure of species i, Pa
q	cross-sectional area, m^2
r	radial coordinate, m
r_M	averaged membrane radius $(r_1 + r_2)/2$, m
r_1	inner membrane (top layer) radius, m
r_2	outer top layer radius, m
r_3	outer membrane radius, m
$\boldsymbol{R}$	gas constant, J $mol^{-1}\ K^{-1}$
t	time, s
T	temperature, K
V	volume, m^3

$\dot{V}$	volumetric flow rate, $m^3 s^{-1}$
V_p	cumulative pore size distribution, $m^3 kg^{-1}$
x_i	mole fraction of species *i*
Δx_i	mole fraction difference of species *i* ($x_2 - x_1$)
z	axial coordinate, m
ε	porosity
η	viscosity, Pa s
τ	tortuosity
Subscripts	
i,j	species in mixture
K	Knudsen
m	mixture
1	inner
2	outer
Superscripts	
e	effective
D	diffusive
0	initial
S	surface
V	viscous
12	transmembrane

The donation of the membranes by Cerasiv GmbH (Plochingen, Germany) and the financial support of Fonds der Chemischen Industrie is gratefully acknowledged. We are grateful to S. Ehlers for the results of mercury porosimetry.

REFERENCES

1. Haynes H. W.: Catal. Rev. – Sci. Eng. *30*, 563 (1988).
2. Krishna R.: Chem. Eng. Sci. *48*, 845 (1993).
3. Mason E. A., Malinauskas A. P.: *Gas Transport in Porous Media: the Dusty Gas Model*. Elsevier, Amsterdam 1983.
4. Novak M., Ehrhardt K., Klusacek K., Schneider P.: Chem. Eng. Sci. *43*, 185 (1988).
5. Bosanquet C. H.: British T. A. Report 507 (1944).
6. Reid R. C., Prausnitz J. M., Poling B. E.: *The Properties of Gases and Liquids*. McGraw–Hill, Singapore 1988.
7. Veldsink J. W., Versteeg G. F., van Swaaij W. P. M.: J. Membrane Sci. *92*, 275 (1994).
8. Uchytil P.: J. Membrane Sci. *97*, 139 (1994).
9. *CRC Handbook of Chemistry and Physics*. CRC Press, Boca Raton 1993.
10. Brenan K. E., Campbell S. L., Petzold L. R.: *Numerical Solutions of Initial-Value Problems in Differential-Algebraic Equations*. Elsevier, New York 1989.
11. Villadsen J. V., Michelsen M. L.: *Solution of Differential Equation Models by Polynomial Approximation*. Prentice-Hall, Englewood Cliffs (NJ) 1978.
12. Tuchlenski A., Uchytil P., Seidel-Morgenstern A.: J. Membrane Sci., submitted.